

Synthesis of $\text{Bi}_2\text{W}_2\text{O}_9$ from an amorphous complex precursor: characterization and evaluation of its photocatalytical properties

A. Martínez-de la Cruz^{a,*}, S. Obregón Alfaro^a, Leticia M. Torres-Martínez^b, I. Juárez Ramírez^b

^aFacultad de Ingeniería Mecánica y Eléctrica, Universidad Autónoma de Nuevo León, Ciudad Universitaria, C.P. 66451, San Nicolás de los Garza, N.L., MEXICO

^bDepartamento de Ecomateriales y Energía, Universidad Autónoma de Nuevo León, Ciudad Universitaria, C.P. 66451, San Nicolás de los Garza, N.L., MEXICO

Bismuth tungstate $\text{Bi}_2\text{W}_2\text{O}_9$ has been synthesized using diethylenetriaminepentaacetic acid (H_5DTPA), an organic chelating agent of metals in an aqueous solution. The formation of the oxide was followed through characterization techniques such as XRD, TGA/DTA, and SEM. The optimum temperature to decompose the organic matrix and to form $\text{Bi}_2\text{W}_2\text{O}_9$ was determined to be around 720 °C. Below this temperature, $\text{Bi}_2\text{W}_2\text{O}_9$ was formed with a high content of Bi_2WO_6 . At 720 °C particles of the $\text{Bi}_2\text{W}_2\text{O}_9$ with a surface area four times higher than that obtained by a solid-state reaction were obtained. The oxide was tested as a photocatalyst on the degradation of aqueous solutions of rhodamine B under VIS radiation. The photodegradation of the dye followed a kinetic first order with an apparent constant, $k = 2.8 \times 10^{-3} \text{ minute}^{-1}$ and $t_{1/2} = 247$ minutes for an aqueous solution of 5 mg l^{-1} of rhodamine B.

Key words: Bismuth tungstate, $\text{Bi}_2\text{W}_2\text{O}_9$, Photocatalysis, Rhodamine B.

Introduction

The study of semiconductor oxides is a promising field due to their potential application in heterogeneous photocatalysis processes to remove hazardous organic compounds from water and to split water to produce hydrogen [1-3]. Several oxides with different crystalline structures have been tested in order to find an efficient photocatalyst. In this sense, the high photocatalytical activity under UV irradiation, low cost, and stability to corrosion processes of the anatase polymorph of TiO_2 has positioned this material as the photocatalyst of excellence for commercial applications [3]. With the purpose to gather solar energy, numerous efforts have been focused on the development of new visible-light induced photocatalysts. In the past, there are many studies that report visible light driven catalytic activity on semiconductor oxides such as $\text{In}_{1-x}\text{Ni}_x\text{TaO}_4$ [4], CaIn_2O_4 [5], InVO_4 [6], BiVO_4 [7], $\gamma\text{-Bi}_2\text{MoO}_6$ [8], etc.

Some of the above mentioned oxides crystallize in the Aurivillius structural-type. Several oxides with this crystalline structure have been studied extensively since its discovery in order to know more about the chemistry of bismuth and its lone pair electrons. The family of mixed bismuth layered oxides that belongs to the homologous series $\text{Bi}_2\text{A}_n\text{O}_{3n+3}$ ($\text{A} = \text{W}$ or Mo) can be visualized as a

special case of the general Aurivillius series of phases [9]. The structural arrangement of these compounds is formed by $(\text{Bi}_2\text{O}_2)^{2+}$ layers interleaved by perovskite-like layers $(\text{A}_n\text{O}_{3n+1})^{2-}$, where n represents the number of perovskite layers presents (typically $n = 1$ or 2 for W , and $n = 1$ for Mo), see Fig. 1.

In previous studies, some molybdates and tungstates with the Aurivillius structure have shown photocatalytical activity under VIS irradiation. In particular, the molybdate

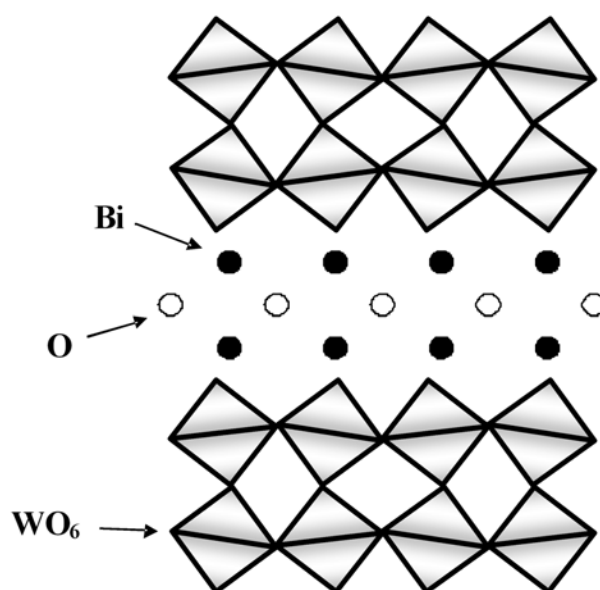


Fig. 1. Crystalline structure of $\text{Bi}_2\text{W}_2\text{O}_9$.

*Corresponding author:
 Tel : +52 (81) 83 29 40 20
 Fax: +52 (81) 83 32 09 04
 E-mail: azael70@yahoo.com.mx

$\gamma\text{-Bi}_2\text{MoO}_6$ showed activity for O_2 -evolution from an aqueous silver nitrate solution [10]. In the same way, its homologous phase Bi_2WO_6 showed photocatalytic activity for H_2 -evolution from an aqueous methanol solution and for O_2 -evolution from an aqueous silver nitrate solution [11]. Although in their early work Kudo and Hiji reported over ten times higher photocatalytic activity on $\text{Bi}_2\text{W}_2\text{O}_9$ than Bi_2WO_6 for H_2 -evolution and O_2 -evolution under UV radiation [11], the second member of the family $\text{Bi}_2\text{W}_n\text{O}_{3n+3}$ has received less attention. Tang and Ye [12] correlated the structural and electronic structure of $\text{Bi}_2\text{W}_2\text{O}_9$ with its photocatalytic properties for the evolution of H_2 and O_2 .

Frequently the solid-state reaction method employed to obtain the photocatalyst leads to materials with poor photocatalytic activity due to the small surface area developed. The so-called soft chemistry methods have shown to be efficient to prepare better catalysts than those synthesized by classical methods. Taking advantage from these methods, Zhang et al. [13] reported the formation of Bi_2WO_6 through a complex organic precursor. In the present study, some improvements to the procedure described by Zhang et al. have been carried out in order to obtain the oxide $\text{Bi}_2\text{W}_2\text{O}_9$. The successful synthesis and characterization of $\text{Bi}_2\text{W}_2\text{O}_9$ will provide an interesting candidate for photocatalytic applications.

Materials and experimental procedures

Synthesis of $\text{Bi}_2\text{W}_2\text{O}_9$

$\text{Bi}_2\text{W}_2\text{O}_9$ was prepared via an amorphous complex precursor by means of a procedure that was described previously for the synthesis of Bi_2WO_6 [13]. 0.0516 mol of diethylenetriaminepentaacetic acid (H_5DTPA) [Aldrich, 99%] and 30 ml of ammonium hydroxide (13 mol l^{-1}) were placed in 300 ml of hot distilled water. After dissolution, 0.006454 mol Bi_2O_3 [Aldrich, 99.9%+] and 0.001075 mol $(\text{NH}_4)_{10}(\text{W}_{12}\text{O}_{41}) \cdot 7\text{H}_2\text{O}$ [Aldrich, 99.9%+] were added. A continuous stirring was necessary at 80°C in order to dissolve all the bismuth oxide. A precursor was obtained by drying the above solution at 80°C for 3 days. The precursor was heated at 600°C for 2 h in order to eliminate the organic components and later to 720°C for 20 h to promote the formation of $\text{Bi}_2\text{W}_2\text{O}_9$.

For comparative purposes, $\text{Bi}_2\text{W}_2\text{O}_9$ was also synthesized by the traditional solid-state reaction between Bi_2O_3 [Aldrich, 99.9%+] and WO_3 [Aldrich, 99.995%]. A stoichiometric mixture was placed in a porcelain crucible and then heated at 800°C for 48 h to obtain the bismuth tungstate.

Sample characterization

Structural characterization was carried out by powder X-ray diffraction using a Bruker D8 Advanced diffractometer with CuK_α radiation doted with a Vantec high speed detector. X-ray diffraction data of samples were collected in the 2θ range of $10\text{-}70^\circ$ with a scan rate of $0.05^\circ/0.05 \text{ s}$. The morphology of the samples

was analyzed by scanning electron microscopy using a JSM JEOL 6490 LV microscope with an accelerating voltage of 20 kV.

Thermogravimetric and differential thermal analyses (TGA/DTA) were performed on a TA Instruments Mod SDT Q600 thermal analyzer. Measurements were carried out under a nitrogen atmosphere with a flux of 100 ml/minute and with a heating rate of $10^\circ\text{C minute}^{-1}$. The surface area of the photocatalysts was determined by N_2 adsorption-desorption measurements using a surface area analyzer, Micromeritics ASAP-2000. The isotherms of adsorption-desorption were evaluated at -196°C after a pretreatment of the sample at 100°C for 2 h. UV-diffuse reflectance spectra of the oxides were measured using a UV-Vis spectrophotometer equipped with an integration sphere (Perkin Elmer Lambda 35).

Photocatalytic reactions

The photochemical reactor employed was a homemade device. It consists of a glass borosilicate beaker surrounded with a water-jacket to maintain the reaction temperature at $25^\circ\text{C} \pm 1^\circ\text{C}$. A Xe lamp of 10,000 K with a luminous flux of 2,100 lm was used as the source of visible light. A minor contribution of UV radiation was observed, but, nearly 90% of this was filtered by the borosilicate container. The photocatalytic activity of $\text{Bi}_2\text{W}_2\text{O}_9$ was evaluated on the reaction of degradation of RhB in aqueous solution. In a glass beaker, 220 ml of RhB solution [5 mg l^{-1}] containing 220 mg of photocatalyst were put in an ultrasonic bath for 15 minutes to eliminate aggregates. The solution was left in the dark for 1 h to ensure the equilibrium adsorption-desorption of the dye on the catalyst surface. After this time, the light source was turned on. During the reaction, samples of 6 ml were taken at given time intervals and then separated through centrifugation (4,000 rpm, 20 minutes). The supernatant solution was decanted and the concentration of RhB was determined through its absorption band maximum (554 nm) using a UV-Vis spectrophotometer (Perkin Elmer Lambda 35).

Results and Discussions

Sample characterization

Starting from the precursor, the formation of the $\text{Bi}_2\text{W}_2\text{O}_9$ phase at low temperatures of calcination was frequently accompanied by Bi_2WO_6 . For this reason, the lowest temperature employed to prepare $\text{Bi}_2\text{W}_2\text{O}_9$ was about 720°C . Nevertheless, even at this temperature a small diffraction peak of the Bi_2WO_6 was observed. This situation seems to be inherent in the thermodynamics of the system $\text{Bi}_2\text{O}_3\text{-WO}_3$ as has been observed previously [14, 15]. Fig. 2 shows the X-ray diffraction pattern of a sample of $\text{Bi}_2\text{W}_2\text{O}_9$ obtained at 720°C using the amorphous complex precursor method. All diffraction lines of $\text{Bi}_2\text{W}_2\text{O}_9$ were identified and assigned according to the JCPDS Card. No. 89-8114. At $2\theta = 28.5^\circ$ a diffraction line associated with the plane [1 3 1] of Bi_2WO_6 was observed as an

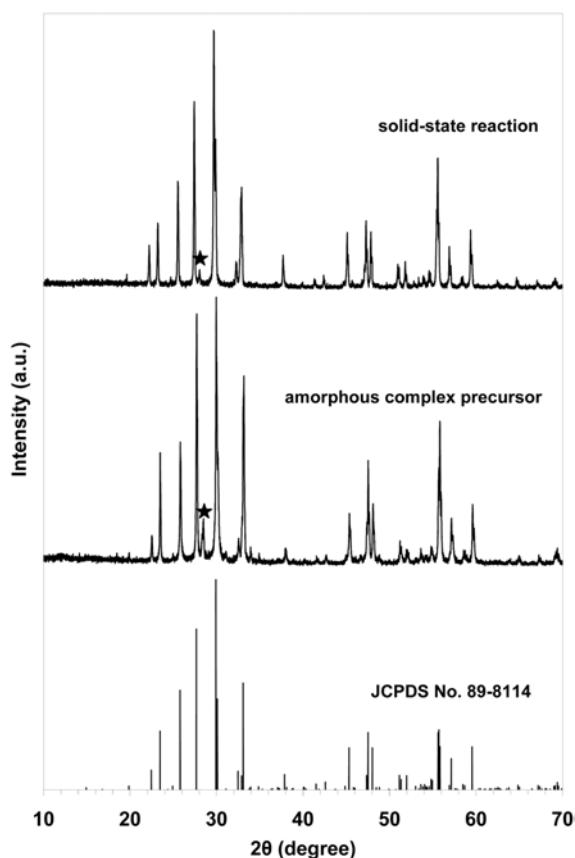


Fig. 2. XRD patterns of $\text{Bi}_2\text{W}_2\text{O}_9$ powders obtained by different routes of synthesis (* peak due to Bi_2WO_6).

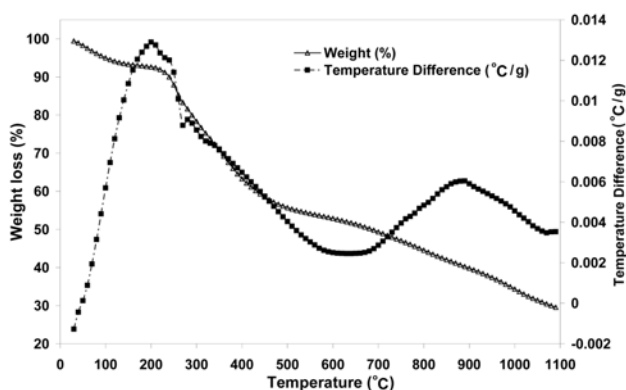


Fig. 3. TGA and DTA analysis of the precursor used to prepare $\text{Bi}_2\text{W}_2\text{O}_9$ by the amorphous complex precursor method.

impurity (JCPDS Card. No. 39-0256). The X-ray diffraction pattern of the sample prepared by a solid state reaction is also shown.

Fig. 3 shows the TGA/DTA plots of the precursor powder in the temperature range 30-1,100 °C. The initial weight loss (~7%) corresponds to water evaporation (~100 °C) due to adsorbed and occluded water on the precursor. The main thermal event takes place between 230-450 °C and corresponds to the burning of both hydrocarbon and amino-groups of the H_3DTPA [13]. The decomposition process of $(\text{NH}_4)_{10}(\text{W}_{12}\text{O}_{41}) \cdot 7\text{H}_2\text{O}$ happens in the temperature interval of 300-400 °C, but

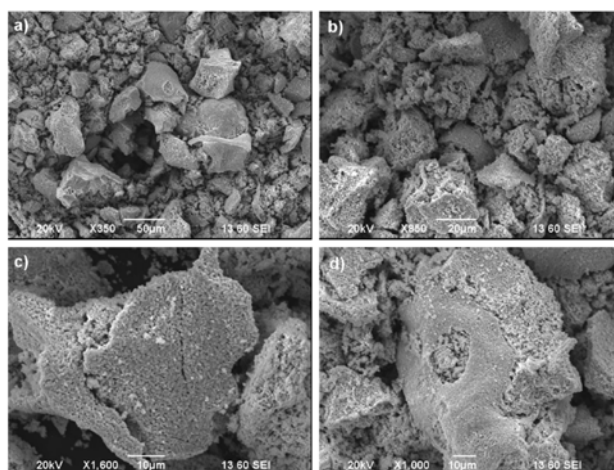


Fig. 4. Morphologies analyzed by SEM of $\text{Bi}_2\text{W}_2\text{O}_9$ powders synthesised by the amorphous complex precursor.

thermal events associated with this process were not observed due to the total decomposition corresponding with a weight loss of 2%. After 450 °C a gradual weight loss is observed due to volatility of the sample and, in a minor proportion by the removal of residual organic material.

The morphology of $\text{Bi}_2\text{W}_2\text{O}_9$ powders obtained by the two routes of synthesis was observed by SEM analysis. A sample prepared by the amorphous complex precursor route at 720 °C, see Fig. 4a-d, showed the presence of small particles less than 1 micrometre in size, such particles are formed into agglomerates which produce a partially sintered porous material. The formation of pores in this material could be related also with the evolution of CO_2 , H_2O and NH_3 gases during the organic matrix decomposition. For comparative purposes, the morphology of $\text{Bi}_2\text{W}_2\text{O}_9$ obtained by a solid state reaction at 800 °C was also observed by SEM. In this case, the presence of agglomerates formed by well sintered large plates 10 micrometres in size was observed, see Fig. 5a-b. A second morphology was observed formed by an agglomerate of semi-ovoid particles with different sizes, see Fig. 5c-d. By EDS analysis it was determined that the large plates had a similar composition to the theoretical $\text{Bi}_2\text{W}_2\text{O}_9$. On the other hand, the semi-ovoid particles corresponded with unreacted tungsten oxide. As was mentioned previously, the formation of $\text{Bi}_2\text{W}_2\text{O}_9$ by different routes of synthesis, including a solid state reaction, is always accompanied by a small quantity of Bi_2WO_6 . The presence of WO_3 is directly related with the Bi_2WO_6 observed by X-ray diffraction. This process can be explained on the basis of the reaction:



An analysis by EDS of different regions of the sample prepared by the amorphous complex precursor method revealed a homogeneous material with a composition near to $\text{Bi}_2\text{W}_2\text{O}_9$. No evidences of the presence of Bi_2WO_6 or WO_3 were found by this technique.

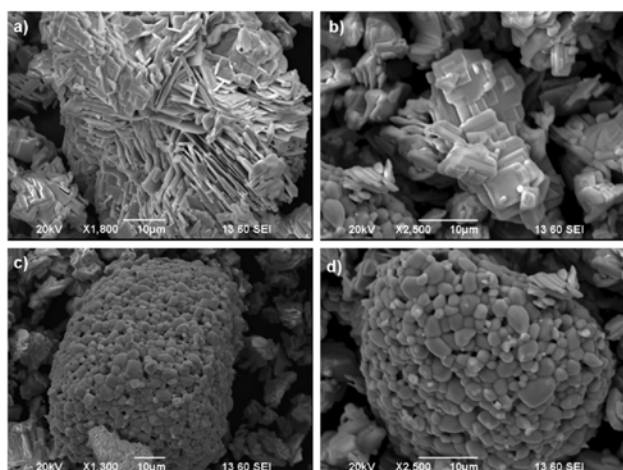


Fig. 5. Morphologies analyzed by SEM of $\text{Bi}_2\text{W}_2\text{O}_9$ powders synthesised by a solid state reaction.

According to the SEM results, the morphology observed in both materials indicates that $\text{Bi}_2\text{W}_2\text{O}_9$ prepared by the amorphous complex precursor route could give a bigger surface area value than the $\text{Bi}_2\text{W}_2\text{O}_9$ prepared by a solid state reaction. Such a situation was confirmed by BET analysis, where surface area values were $0.9 \text{ m}^2/\text{g}$ (amorphous complex precursor), and $0.22 \text{ m}^2/\text{g}$ for the sample prepared by a solid-state reaction. The latter value is similar to that reported in a previous study [12]. On the basis of these results, using the H_3DTPA as a chelating agent, a material with a surface area value four times higher than that prepared by conventional methods was obtained.

Photocatalytic activity

The photocatalytic activity of $\text{Bi}_2\text{W}_2\text{O}_9$ was evaluated by degradation of rhodamine B in aqueous solution under visible light irradiation. The temporal evolution of spectral changes during the photodegradation process of RhB by $\text{Bi}_2\text{W}_2\text{O}_9$ synthesized through the amorphous complex precursor method is displayed in Fig. 6. The strong absorption band of RhB located at 554 nm is due to the presence of four ethylated groups on the dye molecule. Visible light irradiation of the $\text{Bi}_2\text{W}_2\text{O}_9/\text{RhB}$ dispersion

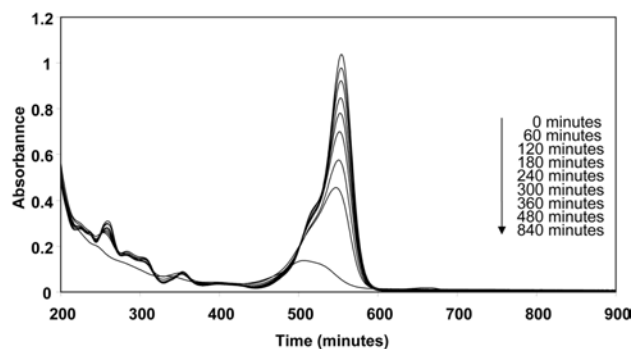


Fig. 6. Absorption changes of RhB solution under photocatalytic process ($440 \text{ mg Bi}_2\text{W}_2\text{O}_9$, prepared at 720°C added into 220 mL of 5 mg l^{-1} RhB solution).

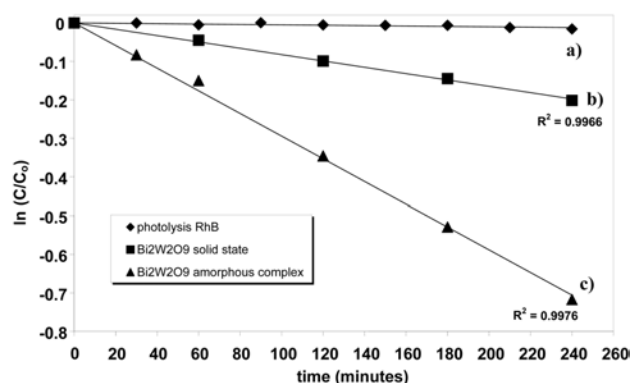


Fig. 7. Changes in RhB concentration during the course of photocatalytic degradation of RhB (5 mg l^{-1}) in the presence of $\text{Bi}_2\text{W}_2\text{O}_9$ (1 g l^{-1}) obtained by two routes of synthesis.

produces a gradual depletion in the absorbance value. This depletion was accompanied by a slight shift towards the blue region only for the sample analyzed for large times (840 minutes). This situation revealed the mechanism followed during the photodegradation of RhB. As is well known, the photodegradation of RhB can happen by two competitive mechanisms: by an attack of $\bullet\text{OH}$ radicals on the aromatic chromophore ring, leading to the degradation of the RhB structure and the reduction of absorption without a wavelength shift; or by a successive de-ethylation from the aromatic rings, causing significant blue wavelength shifts according to the formation of the different de-ethylated rhodamines. According with the spectral changes observed in Fig. 6, it seems to be clear that the predominant mechanism of the photodegradation of RhB is by attack of the aromatic chromophore ring over de-ethylated processes.

Fig.7 shows the temporal evolution of the $\ln(C/C_0)$ when $\text{Bi}_2\text{W}_2\text{O}_9$ synthesized by two different routes were employed. In the first instance, under our experimental conditions the dye did not present a photolysis process induced by the irradiation source (7a). When the bismuth tungstate was dispersed in an aqueous solution of RhB it was able to bleach the solution of dye (7b and 7c). The kinetic data of Fig. 7 can be adjusted in accord with a first-order reaction equation, $\ln(C/C_0) = -kt$, where C_0 and C are the concentrations of RhB before and after the irradiation (mg l^{-1}), t the time (minutes) and k is the apparent reaction rate constant (minutes^{-1}). For a RhB solution with an initial concentration of 5 mg l^{-1} containing 1 g l^{-1} of $\text{Bi}_2\text{W}_2\text{O}_9$ obtained at 720°C , the value of k is $2.8 \times 10^{-3} \text{ minutes}^{-1}$. On the basis of this model, the half-life period of RhB, $t_{1/2}$, was found to be 247 minutes.

The oxide prepared by the amorphous complex precursor method was a four times more efficient photocatalyst than that prepared by a solid state reaction. This relation is in agreement with the surface area relation obtained for each oxide, which was four times greater in the sample obtained using the precursor method.

As is well known, the degradation of a dye by light irradiation can happen by three mechanisms: a) by means

of a photolysis process induced by luminous energy that provides a source, b) by means of a true heterogeneous photocatalysis where the promotion of an electron from the valence band to the conduction band by light irradiation produces active sites for the oxidation of the dye on the valence band of the semiconductor and, c) by means of a photosensitization process where the light is an electron from the dye and then it is injected into the conduction band of the semiconductor with the concomitant oxidation of the dye.

The photocatalytic degradation of RhB by $\text{Bi}_2\text{W}_2\text{O}_9$ takes place by a photosensitization process. This statement is supported by some physical characteristics of the semiconductor $\text{Bi}_2\text{W}_2\text{O}_9$ and the dye employed, i.e. RhB. Firstly, the band gap of the $\text{Bi}_2\text{W}_2\text{O}_9$ near to 3.0 eV limits the absorption of radiation from the visible spectrum (> 400 nm). In fact, in a previous study, a negligible photocatalytic activity to H_2 - and O_2 -evolution has been observed on experiments with visible irradiation [11]. On the other hand, the RhB is a xantane dye widely known as a photosensitizer on TiO_2 and other oxides [3]. The maximum of absorption of RhB is located at 554 nm, so, the energy provide from the Xe lamp is enough for the photosensitization process.

Conclusions

$\text{Bi}_2\text{W}_2\text{O}_9$ has been synthesized successfully through a method that involves an amorphous complex precursor. By this method, a porous material was obtained with a very small particle size, less than 1 micrometre, which leads to the formation of agglomerates. Although the surface area obtained for this material was low, ~ 1 m^2/g , this value was four times more than that obtained by a classical solid state reaction. The method employed for the synthesis provides a material with possible applications in catalysis and photocatalysis fields. The material prepared was able to act as photocatalyst in the degradation of aqueous solutions of rhodamine B under visible irradiation.

The photodegradation process of RhB was carried out by means of a photosensitization process.

Acknowledgements

We wish to thank Universidad Autónoma de Nuevo León (UANL) for its support through the project PAICYT-2007. We also thank Departamento de Ecomateriales y Energía of Facultad de Ingeniería Civil (UANL) for its assistance in the materials characterization.

References

1. J.M. Herrmann, *Top. Catal.* 34 (2005) 49-65.
2. D. Chatterjee and S. Dasgupta, *J. Photoch. Photobio. C* 6 (2005) 186-205.
3. M. Ni, M.K.H. Leung, D.Y.C. Leung and K. Sumathy, *Renew. Sust. Energ. Rev.* 11 (2007) 401-425.
4. Z.G. Zou, J.H. Ye, K. Sayama and H. Arakawa, *Nature* 414 (2001) 625-627.
5. J.W. Tang, Z.G. Zou and J.H. Ye, *Chem. Mater.* 16 (2004) 1644-1649.
6. Z. Zou, J. Ye, K. Sayama and H. Arakawa, *Chem. Phys. Lett.* 333 (2001) 57-62.
7. A. Kudo, K. Omori and H. Kato, *J. Am. Chem. Soc.* 121 (1999) 11459-11467.
8. H. Kato, M. Hori, R. Kouta, Y. Shimodaira and A. Kudo, *Chem. Lett.* 33 (2004) 1348-1349.
9. D.A. Jefferson, J. Gopalakrishnan and A. Ramanan, *Mater. Res. Bull.* 17 (1982) 269-276.
10. Y. Shimodaira, H. Kato, H. Kobayashi and A. Kudo, *J. Phys. Chem. B* 110 (2006) 17790-17797.
11. A. Kudo and S. Hiji, *Chem. Lett.* 28 (1999) 1103-1104.
12. J. Tang and J. Ye, *J. Mater. Chem.* 15 (2005) 4246-4251.
13. S. Zhang, C. Zhang, Y. Man and Y. Zhu, *J. Solid State Chem.* 179 (2006) 62-69.
14. M. Kudo, H. Ohkawa, W. Sugimoto, N. Kumada, Z. Liu, O. Terasaki and Y. Sugahara, *Inorg. Chem.* 42 (2003) 4479-4484.
15. R.E. Schaak and T.E. Mallouk, *Chem. Commun.* 7 (2002) 706-707.